medRxiv preprint doi: https://doi.org/10.1101/2020.08.25.20182162; this version posted August 31, 2020. The copyright holder for this preprint (which was not certified by peer review) is the author/funder, who has granted medRxiv a license to display the preprint in perpetuity.
It is made available under a CC-BY-NC-ND 4.0 International license .

Optimising social mixing strategies to mitigate the impact of COVID-19 in six European countries: a mathematical modelling study

Romain Ragonnet[1,*], Guillaume Briffoteaux[2,3], Bridget M. Williams[1], Julian Savulescu[4], Matthew Segal[1], Milinda Abayawardana[1], Rosalind M. Eggo[5], Daniel Tuyttens[2], Nouredine Melab[3], Ben J. Marais[6], Emma S. McBryde[7], James M. Trauer[1].

[1]School of Public Health and Preventive Medicine, Monash University, Melbourne, Australia
[2]Mathematics and Operational Research Department, University of Mons, Belgium
[3]Université de Lille, CNRS CRIStAL, Inria Lille, France
[4]University of Oxford, Murdoch Children's Research Institute, Oxford, UK
[5]Centre for Mathematical Modelling of Infectious Diseases, London School of Hygiene & Tropical Medicine, London, UK
[6]Marie Bashir Institute for Infectious Diseases and Biosecurity, University of Sydney, Sydney, Australia
[7]Australian Institute of Tropical Health and Medicine, James Cook University, Townsville, Australia
*Correspondence to romain.ragonnet@monash.edu

ABSTRACT

Background: If SARS-CoV-2 elimination is not feasible, strategies are needed to minimise the impact of COVID-19 in the medium-to-long term, until safe and effective vaccines can be used at the population-level.
Methods: Using a mathematical model, we identified contact mitigation strategies that minimised COVID-19-related deaths or years of life lost (YLLs) over a time-horizon of 15 months, using an intervention lasting six or 12 months, in Belgium, France, Italy, Spain, Sweden and the UK. We used strategies that either altered age- or location-specific contact patterns. The optimisation was performed under the constraint that herd immunity should be achieved by the end of the intervention period if post-infection immunity was persistent. We then tested the effect of waning immunity on the strategies.
Findings: Strategies of contact mitigation by age were much more effective than those based on mitigation by location. Extremely stringent contact reductions for individuals aged over 50 were required in most countries to minimise deaths or YLLs. The median final proportion of the population ever-infected with SARS-CoV-2 after herd immunity was reached ranged between 30% and 43%, depending on the country and intervention duration. Compared to an unmitigated scenario, optimised age-specific mitigation was predicted to avert over 1 million deaths across the six countries. The optimised scenarios assuming persistent immunity resulted in comparable hospital occupancies to that experienced during the March-April European wave. However, if immunity was short-lived, high burdens were expected without permanent contact mitigation.
Interpretation: Our analysis suggests that age-selective mitigation strategies can reduce the mortality impacts of COVID-19 dramatically even when significant transmission occurs. The stringency of the required restrictions in some groups raises concerns about the practicality of these strategies. If post-infection immunity was short-lived, solutions based on a mitigation period designed to increase population immunity should be accompanied with ongoing contact mitigation to prevent large epidemic resurgence.

NOTE: This preprint reports new research that has not been certified by peer review and should not be used to guide clinical practice.

medRxiv preprint doi: https://doi.org/10.1101/2020.08.25.20182162; this version posted August 31, 2020. The copyright holder for this preprint (which was not certified by peer review) is the author/funder, who has granted medRxiv a license to display the preprint in perpetuity.
It is made available under a CC-BY-NC-ND 4.0 International license .

Introduction

The rapid spread of SARS-CoV-2 has resulted in millions of cases of COVID-19 and hundreds of thousands of deaths. The speed of spread and the severity of illness, particularly in older people, have resulted in a global crisis that overwhelmed health care systems and induced economic hardship in many settings.

In an effort to reduce transmission and limit these negative effects, many governments have implemented severe restrictions on population movement and social mixing. These have varied in scope and stringency [1], and have included 'stay at home' orders, travel restrictions and school and business closures. Although these measures, combined with extensive testing, strict quarantine and contact tracing with isolation, have been successful in reducing transmission in many countries, the adverse community-wide effects of these restrictions have been severe. Evidence from the United Kingdom (UK) suggests restrictions have had negative effects on mental health [2, 3], and non-COVID-19 health through delays in diagnostic services [4].

In the absence of a vaccine, there are very few alternative approaches to combating the pandemic; each associated with major drawbacks which should be objectively quantified. Although elimination of infection has been successful in some settings, attempts to ease restrictions have often resulted in epidemic recurrence. As long as a large proportion of the population remains susceptible to SARS-CoV-2 infection, populations will remain at high risk of resurgencences of transmission. Reaching a level of post-infection immunity in the population that results in the effective reproduction number remaining below 1 (also called "herd immunity") can be part of a strategy to minimise population health impacts over the medium-to-long term [5].

As countries begin to lift movement and contact restrictions, it is necessary to determine which restrictions that, if lifted, result in fewer cases, hospitalisations and deaths in the medium and long term than a relaxation of measures in all ages and locations.

Countries such as Sweden have tried to minimise the health impact of the disease with less restrictive measures, to slow transmission while shielding those at greatest risk [6]. However, Swedish authorities have acknowledged errors in implementation, particularly around infection prevention in aged residential care facilities [7]. The UK also initially aimed for a limited lockdown with shielding of at-risk groups, but changed course after modelling estimates found that without drastic measures, hundreds of thousands of deaths would be expected [8].

We present an optimisation analysis that aims to identify strategies of social contact restrictions that result in non-vaccine herd immunity within six or 12 months while minimising the number of COVID-19-related deaths or years of life lost (YLLs) over a time-horizon of 15 months in six highly affected countries: Belgium, France, Italy, Spain, Sweden and the UK.

Methods

Overall approach

We used a deterministic compartmental model to simulate SARS-CoV-2 transmission in the six countries analysed. The countries were the six highest ranked countries in COVID-19 deaths per capita as reported by the World Health Organization (WHO) on 15th July 2020, excluding countries of less than one million people. After calibrating the model using local data, we manipulated social mixing patterns for a fixed intervention period of six or 12 months. During this phase, we identified the changes to contact

medRxiv preprint doi: https://doi.org/10.1101/2020.08.25.20182162; this version posted August 31, 2020. The copyright holder for this preprint (which was not certified by peer review) is the author/funder, who has granted medRxiv a license to display the preprint in perpetuity.
It is made available under a CC-BY-NC-ND 4.0 International license .

patterns that would minimise COVID-19-related mortality measured as deaths or years of life lost over a time-horizon of 15 months, while ensuring that all restrictions could be relaxed after the intervention phase without resurgence. We also explored scenarios of waning immunity to project the future epidemics under the identified optimal plans.

Transmission model

Our model explicitly simulated six infection states using a susceptible compartment, two pre-disease compartments (including one presymptomatic infectious), two disease states (early and late stages) and a recovered compartment (Supplementary Section 1.2). Disease states were stratified according to disease severity, as well as estimated detection and hospitalisation fractions.

We employed age-specific parameter values to characterise susceptibility to infection, disease severity and risk of death (Supplementary Table S4). We used previously published age-specific contact matrices by location (home, schools, workplace and other locations) to inform heterogeneous mixing by age [9].

Social distancing was implemented through physical and micro-distancing. Physical distancing reduced the location-specific contact rates in schools, workplaces, and locations other than schools, workplaces and homes (referred to as "other locations" hereafter). Micro-distancing reduced the transmission probability in non-household contacts, reflecting preventive measures that individuals may take to reduce the per-contact transmission probability, such as keeping a greater distance, hygienic measures, and wearing masks.

Under the base-case assumption of persistent immunity, recovered individuals were assumed to be protected against future infection for the duration of the simulations. Four scenarios of waning immunity were also considered by assuming that recovered individuals became susceptible to reinfection after an average duration of six or 24 months, with or without reduction in disease severity during repeat SARS-CoV-2 infections (Supplementary Sections 1.2, 1.4). Births and non-COVID-19-related deaths were not modelled.

Model fitting and simulation phases

We fitted the model to observed numbers of confirmed cases and hospitalisations over time (Supplementary Section 2). Fitted parameters included those governing transmission, disease severity and the time-variant profiles of case detection and micro-distancing. Our model and its calibrations are presented in details in the Supplement and the code used to implement the model is publicly available on Github [10]. Our simulations were divided into three successive phases (Figure 1). In Phase 1 we modelled the preceding SARS-CoV-2 epidemics and included social distancing measures in place in each country until 31st July 2020 (Figure S4). In Phase 2 the model was run using the same epidemiological parameters and detection profile as during Phase 1, but micro-distancing was discontinued and social mixing interventions were optimised for six or 12 months, before being lifted in Phase 3.

Optimising contact patterns

We used two different indicators to represent the disease impact in separate optimisations: the number of COVID-19-related deaths and the number of YLLs due to

medRxiv preprint doi: https://doi.org/10.1101/2020.08.25.20182162; this version posted August 31, 2020. The copyright holder for this preprint (which was not certified by peer review) is the author/funder, who has granted medRxiv a license to display the preprint in perpetuity.
It is made available under a CC-BY-NC-ND 4.0 International license .

COVID-19-related deaths. The number of YLLs was estimated by summing the expected number of remaining years that individuals would have lived if they had not died from COVID-19, using the country-specific life-expectancy values by age reported by the United Nations [11]. The two objective functions were calculated over a time-horizon of 15 months covering Phases 2 and 3. Two types of mitigation strategies were explored. First, we allowed contact rates to vary by age by applying age-specific mixing factors to the original contact matrix (Supplementary Section 3.2). A mixing factor is defined as the relative opportunity of social contact that an individual of a given age has, compared to the pre-COVID-19 era. Therefore, the relative contact rate of one age category with respect to another is calculated as the product of the mixing factors of the age-groups of the infectious and susceptible individuals. In a separate set of analyses, we considered reductions in social mixing by location where the decision variables were scaling factors applying to the location-specific contact rates (Supplementary Section 3.2).

All decision variables were assumed to be bounded between zero and one and the optimisation was also constrained to solutions in which the number of incident cases did not increase after the mitigation phase. As the optimisation tasks were computationally-expensive, the searches were performed using a parallel Genetic Algorithm where the newly generated candidate strategies were evaluated in parallel on multiple CPUs [12].

Sensitivity analyses

In order to test the sensitivity of the objective functions to alterations of each optimised variable, we calculated the marginal variable deviation from the optimum that would cause an excess of 20 deaths per million people (or 1000 YLLs per million people when minimising YLLs) as compared to the optimum (Supplementary Section 4.3). An additional sensitivity analysis was performed considering that the age-specific mixing factors could not be reduced below a minimum mixing threshold (Supplementary Section 5.1).

Results

Optimisation results

The posterior parameter estimates and the inferred time-variant profile of case detection are presented in Supplementary Section 2.4 and 2.5 for the six countries. The model fits are shown in Figure 2. For each of the countries, age-specific mixing restrictions resulted in fewer deaths and YLLs than location-specific mixing reductions (Table 1 and Supplementary Table S8), although both generated considerably fewer deaths and YLLs compared to an unmitigated scenario. In both cases the longer intervention duration led to lower deaths and YLLs (Table 1). The number of additional deaths occurring during Phases 2 and 3 was significantly lower than the number of deaths that had occurred before 1st August 2020 in all countries.

For all countries, contacts of older adults were restricted most, while contacts of individuals aged between 15 and 49 years old were unchanged for optimisation of deaths or YLLs (Figure 3). Contacts involving children and adolescents were also maintained at or near 100% in most countries under the optimised scenarios. The optimal mitigation profile of Sweden presented significant differences compared to that of the other countries, in that higher contributions to social mixing were required of the older age-groups in order to achieve herd immunity. This finding was likely because the inferred risk of transmission per contact was lower than for the other countries in the model (Figure

medRxiv preprint doi: https://doi.org/10.1101/2020.08.25.20182162; this version posted August 31, 2020. The copyright holder for this preprint (which was not certified by peer review) is the author/funder, who has granted medRxiv a license to display the preprint in perpetuity.
It is made available under a CC-BY-NC-ND 4.0 International license .

S8). The objective functions (deaths or YLLs) were highly sensitive to small perturbations in the mixing contributions of young-to-middle-age adults considered in the sensitivity analyses. In contrast, the contact rates involving children and adolescents could deviate significantly from the optimal plan without compromising the objective functions to a large extent.

Optimising for YLLs, rather than deaths, resulted in a larger decrease in contacts needed in the 50-54-year-old age-group across all scenarios. These restrictions were compensated for through a relaxation of restrictions for older age-groups or for young children. The patterns of optimal mixing by age were relatively similar between the 6-month and 12-month mitigation strategies, although the longer scenario featured slightly greater contact reductions. In Spain under the 12-month mitigation phase, contacts involving children were restricted more than in the other countries. This may be explained by the relatively high contact rates from children to elderly individuals in Spanish households, compared to other countries [9].

Stronger restrictions were consistently imposed on the age-groups at highest risk of death, although contact reductions were sometimes also recommended for low-risk age-groups. For example, significant restrictions were recommended for 20-24 year-olds in the UK under the 12-month mitigation scenario, which can be explained by the fact that this age-group is the greatest source of contacts for the 75+ age-group among all young to middle-aged adults in the UK (Figure S10).

In the sensitivity analyses considering minimum mixing thresholds, we found that the two objective functions increased roughly linearly, as the minimum mixing threshold was raised (Figure S11). Considering a threshold of 20%, we predicted that herd immunity could still be achieved with a total number of deaths after 31st July 2020 that would be lower or similar to the death toll observed before this date in all countries except the UK.

Considering optimised mitigation by location, social interactions in workplaces were maintained at the highest level in the six countries regardless of the scenario considered (Figure 4). Contacts occurring in schools also maintained very high frequencies in all countries, although significant variability was allowed around these contact rates without compromising outcomes. We noted one exception in Spain under the 12-month mitigation phase, for which the restriction of school contacts proved to be greater than that of other countries, reminding the findings emerging from the optimisation by age. Since age-specific mitigations were more effective than location, we present further results only on age-specific mitigations, although location-specific results are provided in the Supplement.

The full age-specific contact matrices resulting from all optimisations are presented in the Supplement for all scenarios (Figures S11 and S12).

Projected epidemics

Considering age-specific mitigation, the optimised epidemics during the mitigation phase had higher peak incidence than during the modelled first waves in most settings (Figure 5). The younger populations were considerably more affected in the optimised wave. This resulted in much lower predicted numbers of deaths during the optimised phase compared with the first wave. The median percentage of the population ever-infected with SARS-CoV-2 after herd immunity was reached ranged between 30% and 43% depending on the country and the scenario considered (Table 2). Further results are given in Supplementary Figure S14 and Figure S15.

Our model projects that under a 6-month mitigation scenario assuming persistent

medRxiv preprint doi: https://doi.org/10.1101/2020.08.25.20182162; this version posted August 31, 2020. The copyright holder for this preprint (which was not certified by peer review) is the author/funder, who has granted medRxiv a license to display the preprint in perpetuity.
It is made available under a CC-BY-NC-ND 4.0 International license .

immunity, herd immunity could be achieved with similar hospital occupancies to those observed in March and April in the six countries (Figure 6). A longer mitigation phase markedly reduced the peak and total hospital burden.

Effect of waning immunity

Using the 6-month age-specific mitigation scenario, we found that under the four tested scenarios of waning immunity a third epidemic wave would occur by the end of 2021 in the absence of further intervention in all countries, except for Sweden where no epidemic resurgence was predicted under the scenarios of 24-month average duration of immunity (Figure 7). We found the duration of post-infection immunity affected the future epidemics much more than the level of protection against severe disease. Under the assumption of a 6-month immunity duration, the predicted deaths and hospitalisations were considerably greater than observed during Phase 1 or Phase 2, although the predicted incidence remained comparable to that of the first two waves.

Finally, we simulated scenarios considering our most pessimistic assumption of waning immunity (six-month duration and no reduction in future disease severity), but applying mild mixing restrictions during Phase 3 (Figure 8). We estimated that the epidemics could be maintained at low levels until the end of 2021 by applying relative mixing reductions of 10% in Sweden, 20% in Belgium, Italy and Spain and 30% in France and in the UK. These mixing reductions were defined as universal reductions relative to the pre-COVID-19 era across all age-groups.

Discussion

Our model suggests that over the medium-to-long term, non-vaccine herd immunity may be achievable with mortality that is considerably lower than has been previously observed if age-specific mixing patterns can be altered to prevent infection of older individuals. We also estimate that this could be achieved while the impact on hospital capacity is maintained below that experienced in the March-April European wave of COVID-19. We also highlight the critical need for improved knowledge around the post-infection immunity duration if such strategies are to be considered.

As countries move toward relaxation of contact and movement restrictions, we quantify the contact patterns that are most likely to result in increased mortality or YLLs, providing guidance on targeted release strategies. While many governments have used mitigation strategies based on location-specific restrictions, such as school or business closures, we demonstrate that strategies considering age-selective restrictions would have a greater impact on the countries' epidemics. Across all six countries included in our analysis, our model suggested that over 1 million deaths could potentially be averted, and over 15 million life-years saved, by employing age-specific mitigation compared to an unmitigated scenario. Such outcomes were obtained by imposing highly stringent contact reductions on individuals aged over 50, while returning interactions involving children and young-to-middle-aged adults to pre-COVID-19 levels in most countries. This age cutoff is lower than considered in previous studies investigating age-based shielding strategies [13, 14].

The stringency of the optimal restrictions on social contacts of people aged 50 years and over raises concerns about the feasibility of achieving the required age-differential mixing. However, our optimisation did not consider micro-distancing (i.e. efforts to reduce transmission risk when social contacts occur). Reducing the per-contact risk

medRxiv preprint doi: https://doi.org/10.1101/2020.08.25.20182162; this version posted August 31, 2020. The copyright holder for this preprint (which was not certified by peer review) is the author/funder, who has granted medRxiv a license to display the preprint in perpetuity.
It is made available under a CC-BY-NC-ND 4.0 International license .

of transmission would imply that contacts would not need to be reduced to the same extent. Nevertheless, even with micro-distancing attempts, it would be impossible to achieve null effective contact rates in some settings, including multigenerational households or aged care homes. This indicates that the optimised number of deaths and YLLs that we present should be interpreted as a representation of what could ideally be achieved under a best-case scenario. Practical implementation would require further analyses and critical consideration of specific strategies. Finally, our analyses considering less extreme restrictions showed that the numbers of deaths would increase significantly compared to the optimised scenarios. However, these would not necessarily exceed the death toll seen in the first epidemic waves, even if age-specific mixing factors of all age-groups could not be reduced below 20%.

The fact that in several age-groups optimal mixing factors were close to 100% suggests that the outcomes may be further improved if the contact rates were allowed to exceed baseline (pre-COVID-19) rates. We anticipate that increased mixing for the young adults compared to baseline mixing could result in even fewer deaths and YLLs, or require a shorter mitigation phase to achieve herd immunity. Such mixing profiles would be associated with a shorter epidemic duration and a higher peak incidence. This would heighten concerns around hospital capacity, although further investigations are needed to quantify the effect of further shifting the distribution of cases towards younger age-groups through such strategies.

It is notable that the final proportions of ever-infected individuals for each of the modelled scenarios in the six countries were between 30 and 43% in all six countries. Academic and public discussion has largely referred to a herd immunity threshold of between 60 and 70% [15–17], a proportion that can be readily estimated from the R_0 under the assumption of homogenous mixing. In reality, individuals differ in how likely they are to contract and transmit SARS-CoV-2. Several other modelling analyses have emerged that incorporate heterogeneity and have suggested lower estimates of the herd immunity threshold [18–22]. In particular, young-to-middle-age individuals, who have high contact rates as well as high infectiousness and susceptibility to infection, contribute disproportionately to transmission, such that removing them from the susceptible pool would also be disproportionately effective. Our findings also have important implications for vaccination strategies, as we estimated the age-specific proportions of recovered individuals after herd immunity was reached. This suggests that age-selective vaccination strategies could also include groups at higher risk of transmission as well as severe outcomes, although more specific works will be required to identify optimal vaccination strategies.

Our main projections were obtained assuming persistent post-infection immunity. Early studies have shown that the majority of people infected with SARS-CoV-2 generate both humoral and cellular immune responses [23–25]. However, insufficient time has elapsed to quantify the extent and duration of this protection, and whether these changes will prevent reinfection, reduce the risk of onward transmission following infection, or modify the severity of future infections. Some studies have shown antibody levels waning over the first three months post-infection, suggesting short-lived immunity [26]. However, other studies have shown neutralising antibodies to persist at protective levels three [27], and even six months post-infection [25], as well as features of robust cellular immunity, including SARS-CoV-2-specific memory lymphocytes with characteristics suggestive of protective immunity at 3 months post-infection [23, 28–30]. Infection has been shown to offer protection against reinfection in non-human primates [31, 32], and a recent outbreak investigation suggests evidence of protection against reinfection

medRxiv preprint doi: https://doi.org/10.1101/2020.08.25.20182162; this version posted August 31, 2020. The copyright holder for this preprint (which was not certified by peer review) is the author/funder, who has granted medRxiv a license to display the preprint in perpetuity.
It is made available under a CC-BY-NC-ND 4.0 International license .

in humans [33]. Although we considered waning immunity under only a limited number of configurations, these highlight the importance of understanding immune effects and persistence to longer-term public health strategies.

We demonstrated that the selected countries' health systems would be overwhelmed and the numbers of deaths would dramatically increase if immunity were to wane rapidly in the absence of any mitigation after the optimised phase. This demonstrates that long-term restrictions would be required under such scenarios, although such restrictions may consist of only mild continuous contact mitigations following the optimised phase. For example, 20% continued reduction in effective contacts would be needed after the optimised phase in Belgium, Spain and Italy to maintain sufficient epidemic control until the end of 2021. Such reductions could be achieved by reducing the number of contacts or the per-contact risk of transmission (or both).

Our analysis raises several ethical questions regarding policy choices in the pandemic. First, it raises the question of whether or not it would be ethical to restrict the freedom of a vulnerable subset of the population or to purposefully infect a lower-risk subgroup, and to do so on the basis of age. Savulescu and Cameron argue that age-selective lockdowns would not constitute unjust discrimination, as it involves treating people differently due to a morally relevant difference: their susceptibility to severe infection [34]. They suggest that restrictions on personal freedoms would be most justified if they bring about benefit to the group whose freedoms are restricted. It is also possible that restriction of freedom of individuals experiencing strict restrictions could be reduced through the use of immunity passports, though these raise further ethical issues [35]. Factors other than age also impact COVID-19 risk [36], and these factors are also important to consider when designing policies, although we do not explicitly account for these other risk factors.

The results for optimising for deaths or for YLLs were largely consistent, but showed some differences. This raises the question of what the optimisation target should be, and a welfare-adjusted life year, such as the quality-adjusted life year, may be preferable. Our analysis did not include the morbidity of illness or possible long-term sequelae of infection. Data on longer term clinical outcomes of COVID-19 remain limited, but suggest that the majority of people who experience mild-moderate infections recover within two to three weeks [37], although some may experience prolonged symptoms [38]. Long-term post-infection sequelae also occur in some patients, with emerging evidence for an increased risk of stroke during COVID-19 illness [39]. However, more data on long-term outcomes following infection will be required to be able to optimise for minimal morbidity.

In addition to the considerations above, there are some technical limitations of our approach. We used previously published synthetic contact matrices in the model which gave a consistent approach across the six countries and allowed location-specific contact rates [9]. The model assumes that mixing patterns in countries are well represented by the mixing matrix and does not include repeated contacts, such as within households. We chose to mitigate the age-specific contact rates by applying a single multiplier to each age-group, whereas more flexibility could be introduced by allowing mixing between particular pairs of age-groups. Given the important uncertainties in the current epidemiological knowledge of SARS-CoV-2, we chose broad ranges of parameter values to inform the most critical aspects of the model, which translated into moderate uncertainty ranges for several epidemiological indicators. However, we believe our approach to handling uncertainty is appropriate to the current stage of the pandemic.

The present work could be refined as further knowledge arises about SARS-CoV-2

medRxiv preprint doi: https://doi.org/10.1101/2020.08.25.20182162; this version posted August 31, 2020. The copyright holder for this preprint (which was not certified by peer review) is the author/funder, who has granted medRxiv a license to display the preprint in perpetuity.
It is made available under a CC-BY-NC-ND 4.0 International license .

epidemiology, especially around the nature and magnitude of post-infection immunity. In addition, alternative optimisation frameworks to the one used in this study could be assessed in an attempt to further improve population outcomes. Finally, future work could include the negative effects of population restrictions more explicitly in order better to address the trade-off between restriction stringency and uncontrolled viral transmission.

Caution is required to interpret the projections reported in this study correctly. It must be noted that the strategies presented here would undoubtedly result in a greater number of COVID-19-induced deaths compared to approaches based on universal stringent restrictions that would occur during outbreaks. Accordingly, the risks and benefits of the presented strategies are to be carefully weighed against those associated with strict lockdowns, which are also known to have serious negative effects [2–4]. Finding the right balance between these types of approaches will likely depend on how long we will have to wait until long-term solutions such as vaccines can be deployed.

In conclusion, we found that strategies can minimise deaths or YLLs over the medium-to-long term while allowing an increase in population mixing if interpersonal contact patterns can be manipulated to prevent transmission to older adults. In particular, modification of contact rates by age is the key factor, although age-independent vulnerabilities will also require consideration. We show the cut-off for contact restriction - analogous to shielding or cocooning - may occur at a younger age than previously assumed. Finally, our findings suggest that strategies combining a phase of age-selective contact restrictions designed to increase population immunity followed by ongoing but mild contact mitigation could maintain transmission at low levels even with waning post-infection immunity.

Acknowledgements

The optimisation experiments presented in this paper were carried out using the Grid'5000 testbed, supported by a scientific interest group hosted by Inria and including CNRS, RENATER and several Universities as well as other organisations (more details at https://www.grid5000.fr).

References

[1] T. Hale, N. Angrist, B. Kira, A. Petherick, T. Phillips, and S. Webster, "Variation in government responses to COVID-19 Version 6.0. Blavatnik School of Government Working Paper.," tech. rep., Blavatnik School of Government, may 2020.

[2] A. S. F. Kwong, R. M. Pearson, M. J. Adams, K. Northstone, K. Tilling, *et al.*, "Mental health during the COVID-19 pandemic in two longitudinal UK population cohorts," *medRxiv*, p. 2020.06.16.20133116, jun 2020.

[3] M. Pierce, H. Hope, T. Ford, S. Hatch, M. Hotopf, and Jothers, "Mental health before and during the COVID-19 pandemic: a longitudinal probability sample survey of the UK population," *The Lancet Psychiatry*, vol. 0, jul 2020.

[4] C. Maringe, J. Spicer, M. Morris, A. Purushotham, E. Nolte, *et al.*, "The impact of the COVID-19 pandemic on cancer deaths due to delays in diagnosis in England, UK: a national, population-based, modelling study," *The Lancet Oncology*, vol. 0, jul 2020.

medRxiv preprint doi: https://doi.org/10.1101/2020.08.25.20182162; this version posted August 31, 2020. The copyright holder for this preprint **(which was not certified by peer review)** is the author/funder, who has granted medRxiv a license to display the preprint in perpetuity.
It is made available under a CC-BY-NC-ND 4.0 International license .

[5] B. J. Marais and T. C. Sorrell, "Pathways to COVID-19 'community protection'," 2020.

[6] The Public Health Agency of Sweden, "COVID-19: The Swedish strategy," jun 2020.

[7] M. Paterlini, "'Closing borders is ridiculous': the epidemiologist behind Sweden's controversial coronavirus strategy," *Nature*, vol. 580, p. 574, apr 2020.

[8] N. M. Ferguson, D. Laydon, G. Nedjati-Gilani, N. Imai, K. Ainslie, *et al.*, "Impact of non-pharmaceutical interventions (NPIs) to reduce COVID-19 mortality and healthcare demand," *Imperial.Ac.Uk*, no. March, pp. 3–20, 2020.

[9] K. Prem, A. R. Cook, and M. Jit, "Projecting social contact matrices in 152 countries using contact surveys and demographic data," *PLoS Computational Biology*, vol. 13, p. e1005697, sep 2017.

[10] J. M. Trauer, R. Ragonnet, M. Segal, M. Abayawardana, and E. McBryde, "AuTuMN Github repository: https://github.com/monash-emu/AuTuMN/tree/opti_project_simulations," 2019.

[11] United Nations, "World Population Prospects 2019."

[12] E.-G. Talbi, *Metaheuristics: From Design to implementation.* John Wiley & Sons, Ltd, 2009.

[13] K. van Zandvoort, C. I. Jarvis, C. Pearson, N. G. Davies, C. C.-. working Group, *et al.*, "Response strategies for COVID-19 epidemics in African settings: a mathematical modelling study," *medRxiv*, 2020.

[14] N. G. Davies, A. J. Kucharski, R. M. Eggo, A. Gimma, W. J. Edmunds, *et al.*, "Effects of non-pharmaceutical interventions on COVID-19 cases, deaths, and demand for hospital services in the UK: a modelling study," *The Lancet Public Health*, vol. 5, pp. e375–e385, jul 2020.

[15] H. E. Randolph and L. B. Barreiro, "Herd Immunity: Understanding COVID-19," may 2020.

[16] K. O. Kwok, F. Lai, W. I. Wei, S. Y. S. Wong, and J. W. Tang, "Herd immunity – estimating the level required to halt the COVID-19 epidemics in affected countries," jun 2020.

[17] N. Popovich and M. Sanger-Katz, "The World Is Still Far From Herd Immunity for Coronavirus - The New York Times," may 2020.

[18] P. V. Brennan and L. P. Brennan, "Susceptibility-adjusted herd immunity threshold model and potential R 0 distribution fitting the observed Covid-19 data in Stockholm," *medRxiv*, 2020.

[19] T. Britton, F. Ball, and P. Trapman, "A mathematical model reveals the influence of population heterogeneity on herd immunity to SARS-CoV-2.," *Science (New York, N.Y.)*, jun 2020.

[20] A. V. Tkachenko, S. Maslov, A. Elbanna, G. N. Wong, Z. J. Weiner, and N. Goldenfeld, "Persistent heterogeneity not short-term overdispersion determines herd immunity to COVID-19," *medRxiv*, 2020.

medRxiv preprint doi: https://doi.org/10.1101/2020.08.25.20182162; this version posted August 31, 2020. The copyright holder for this preprint (which was not certified by peer review) is the author/funder, who has granted medRxiv a license to display the preprint in perpetuity.
It is made available under a CC-BY-NC-ND 4.0 International license .

[21] R. Aguas, R. M. Corder, J. G. King, G. Gonçalves, M. U. Ferreira, and M. M. Gabriela Gomes, "Herd immunity thresholds for SARS-CoV-2 estimated from unfolding epidemics," *medRxiv*, 2020.

[22] M. G. M. Gomes, R. M. Corder, J. G. King, K. E. Langwig, C. Souto-Maior, *et al.*, "Individual variation in susceptibility or exposure to SARS-CoV-2 lowers the herd immunity threshold.," *medRxiv : the preprint server for health sciences*, 2020.

[23] L. Ni, F. Ye, M. L. Cheng, Y. Feng, Y. Q. Deng, *et al.*, "Detection of SARS-CoV-2-Specific Humoral and Cellular Immunity in COVID-19 Convalescent Individuals," *Immunity*, vol. 52, pp. 971–977.e3, jun 2020.

[24] L. Grandjean, A. Saso, A. Ortiz, T. Lam, J. Hatcher, *et al.*, "Humoral Response Dynamics Following Infection with SARS-CoV-2," *medRxiv*, p. 2020.07.16.20155663, jul 2020.

[25] J. Wu, B. Liang, C. Chen, H. Wang, Y. Fang, *et al.*, "SARS-CoV-2 infection induces sustained humoral immune responses in convalescent patients following symptomatic COVID-19 Correspondence," *medRxiv*, p. 2020.07.21.20159178, jul 2020.

[26] F. J. Ibarrondo, J. A. Fulcher, D. Goodman-Meza, J. Elliott, C. Hofmann, *et al.*, "Rapid Decay of Anti–SARS-CoV-2 Antibodies in Persons with Mild Covid-19," *New England Journal of Medicine*, 2020.

[27] A. Wajnberg, F. Amanat, A. Firpo, D. R. Altman, M. J. Bailey, *et al.*, "SARS-CoV-2 infection induces robust, neutralizing antibody responses that are 1 stable for at least three months 2 3," *medRxiv*, p. 2020.07.14.20151126, jul 2020.

[28] L. B. Rodda, J. Netland, L. Shehata, K. B. Pruner, P. A. Morawski, *et al.*, "Functional SARS-CoV-2-specific immune memory persists after mild COVID-19," *medRxiv*, p. 2020.08.11.20171843, aug 2020.

[29] A. Grifoni, D. Weiskopf, S. I. Ramirez, J. Mateus, J. M. Dan, *et al.*, "Targets of T Cell Responses to SARS-CoV-2 Coronavirus in Humans with COVID-19 Disease and Unexposed Individuals," *Cell*, vol. 181, pp. 1489–1501.e15, jun 2020.

[30] T. Sekine, A. Perez-Potti, O. Rivera-Ballesteros, K. Straling, J.-B. Gorin, *et al.*, "Robust T cell immunity in convalescent individuals with asymptomatic or mild COVID-19," *bioRxiv*, p. 2020.06.29.174888, aug 2020.

[31] A. Chandrashekar, J. Liu, A. J. Martinot, K. McMahan, N. B. Mercado, *et al.*, "SARS-CoV-2 infection protects against rechallenge in rhesus macaques," *Science*, p. eabc4776, may 2020.

[32] W. Deng, L. Bao, J. Liu, C. Xiao, J. Liu, *et al.*, "Primary exposure to SARS-CoV-2 protects against reinfection in rhesus macaques.," *Science (New York, N.Y.)*, jul 2020.

[33] A. Addetia, K. H. Crawford, A. Dingens, H. Zhu, M.-L. Huang, *et al.*, "Neutralizing antibodies correlate with protection from SARS-CoV-2 in humans during a 1 fishery vessel outbreak with high attack rate 2 3," *medRxiv*, p. 2020.08.13.20173161, aug 2020.

medRxiv preprint doi: https://doi.org/10.1101/2020.08.25.20182162; this version posted August 31, 2020. The copyright holder for this preprint **(which was not certified by peer review)** is the author/funder, who has granted medRxiv a license to display the preprint in perpetuity.
It is made available under a CC-BY-NC-ND 4.0 International license .

[34] J. Savulescu and J. Cameron, "Why lockdown of the elderly is not ageist and why levelling down equality is wrong," *Journal of medical ethics*, vol. 0, pp. 1–5, jun 2020.

[35] R. C. H. Brown, J. Savulescu, B. Williams, and D. Wilkinson, "Passport to freedom? Immunity passports for COVID-19," *Journal of Medical Ethics*, pp. medethics–2020–106365, aug 2020.

[36] E. J. Williamson, A. J. Walker, K. Bhaskaran, S. Bacon, C. Bates, *et al.*, "OpenSAFELY: factors associated with COVID-19 death in 17 million patients," *Nature*, 2020.

[37] M. W. Tenforde, E. Billig Rose, C. J. Lindsell, N. I. Shapiro, D. C. Files, *et al.*, "Characteristics of Adult Outpatients and Inpatients with COVID-19 — 11 Academic Medical Centers, United States, March–May 2020," *MMWR. Morbidity and Mortality Weekly Report*, vol. 69, pp. 841–846, jul 2020.

[38] E. Mahase, "Covid-19: What do we know about "long covid"?," jul 2020.

[39] A. E. Merkler, N. S. Parikh, S. Mir, A. Gupta, H. Kamel, *et al.*, "Risk of Ischemic Stroke in Patients with Coronavirus Disease 2019 (COVID-19) vs Patients with Influenza," *JAMA Neurology*, 2020.

medRxiv preprint doi: https://doi.org/10.1101/2020.08.25.20182162; this version posted August 31, 2020. The copyright holder for this preprint **(which was not certified by peer review)** is the author/funder, who has granted medRxiv a license to display the preprint in perpetuity.
It is made available under a CC-BY-NC-ND 4.0 International license .

Country	Mitigation phase	Deaths before 1 Aug 2020 (thousands)		Deaths from 1 Aug 2020 (thousands)			YLLs before 1 Aug 2020 (thousands)	YLLs from 1 Aug 2020 (thousands)		
		Model prediction	WHO report	Unmitigated	Optimised		Model prediction	Unmitigated	Optimised	
					Minimising deaths	Minimising YLLs			Minimising deaths	Minimising YLLs
Belgium	6 months	4.6 (2.5-8.5)	9.8	22.3 (15.9-32.3)	1.9 (1.5-3.0)	2.0 (1.4-6.5)	108 (59-180)	447 (306-574)	114 (82-143)	84 (64-156)
	12 months				0.8 (0.6-1.3)	0.8 (0.5-1.2)			36 (23-52)	29 (19-41)
France	6 months	27.2 (15.9-43.7)	30.1	260.6 (201.3-334.6)	7.5 (6.0-11.1)	7.7 (6.0-11.8)	425 (250-683)	4053 (3309-4504)	268 (240-313)	256 (230-308)
	12 months				5.8 (4.1-9.7)	6.7 (4.8-10.5)			309 (233-373)	216 (165-270)
Italy	6 months	40.9 (26.5-65.5)	35.1	304.2 (227.8-398.2)	11.7 (9.2-31.0)	19.1 (15.5-47.6)	635 (440-1060)	4291 (3645-5172)	514 (451-726)	476 (416-863)
	12 months				6.9 (5.2-12.4)	7.9 (5.8-13.8)			385 (314-528)	339 (277-471)
Spain	6 months	32.4 (18.5-62.7)	28.5	189.5 (141.6-269.1)	8.2 (6.0-31.4)	8.8 (6.3-32.7)	512 (312-812)	2978 (2423-3526)	253 (219-597)	242 (209-609)
	12 months				4.5 (3.1-6.1)	4.8 (3.2-6.5)			191 (141-231)	172 (125-210)
Sweden	6 months	6.3 (2.7-10.6)	5.7	23.6 (11.6-35.9)	4.9 (4.0-7.9)	5.8 (4.8-8.3)	108 (54-166)	397 (197-547)	227 (154-307)	214 (150-286)
	12 months				1.2 (0.8-1.8)	2.5 (1.6-3.8)			101 (49-152)	74 (38-112)
United Kingdom	6 months	31.4 (15.3-53.1)	46.0	252.5 (189.3-324.3)	8.5 (6.9-12.0)	8.9 (7.3-12.4)	608 (304-987)	3985 (3111-4814)	307 (260-396)	281 (241-369)
	12 months				6.2 (4.2-9.7)	6.5 (4.4-9.9)			245 (173-316)	219 (155-286)

Table 1. Predicted numbers of deaths and years of life lost
Optimisation by age under the assumption of persistent immunity. Numbers are presented in thousands of deaths and thousands of YLLs as median and central 95% credible intervals. YLLs: Years of life lost.

Country	Mitigation phase	Proportion of recovered individuals at the end of the optimised mitigation phase (%)	
		Minimising deaths	Minimising YLLs
Belgium	6 months	39.2 (33.9 - 46.8)	35.0 (27.8 - 43.3)
	12 months	30.6 (26.4 - 38.8)	29.8 (26.0 - 36.9)
France	6 months	36.5 (31.9 - 41.9)	34.8 (30.3 - 40.0)
	12 months	30.8 (26.1 - 36.6)	31.6 (26.5 - 37.7)
Italy	6 months	37.0 (32.1 - 40.4)	36.0 (30.9 - 39.4)
	12 months	33.3 (29.3 - 36.6)	33.8 (29.5 - 37.3)
Spain	6 months	36.7 (29.0 - 41.1)	36.5 (28.9 - 40.9)
	12 months	33.4 (27.3 - 37.4)	33.4 (27.3 - 37.5)
Sweden	6 months	42.6 (20.6 - 52.0)	42.6 (20.2 - 52.2)
	12 months	32.5 (19.0 - 40.4)	34.1 (19.5 - 43.0)
UK	6 months	42.8 (38.6 - 47.5)	42.7 (38.5 - 47.4)
	12 months	36.9 (32.1 - 42.7)	38.0 (33.4 - 43.6)

Table 2. Proportions of recovered individuals at the end of the optimised mitigation phase
Optimisation by age under the assumption of persistent immunity. Numbers are presented as median and central 95% credible intervals. Herd immunity was reached by the end of the mitigation phase. YLLs: Years of life lost.

medRxiv preprint doi: https://doi.org/10.1101/2020.08.25.20182162; this version posted August 31, 2020. The copyright holder for this preprint (which was not certified by peer review) is the author/funder, who has granted medRxiv a license to display the preprint in perpetuity.
It is made available under a CC-BY-NC-ND 4.0 International license .

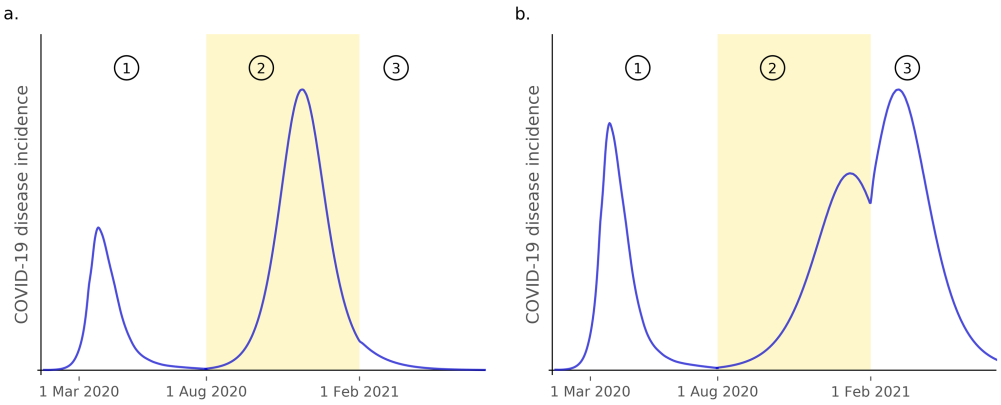

Figure 1. Illustration of the three simulation phases
Numbered circles indicate the different phases: capturing past dynamics (1), manipulating social mixing to achieve herd immunity with minimum COVID-19 impacts (2, highlighted with yellow background), testing for epidemic resurgence (3). Panel a. shows an example simulation where herd immunity was reached by the end of Phase 2, whereas Panel b. shows a configuration that failed to achieve herd immunity.

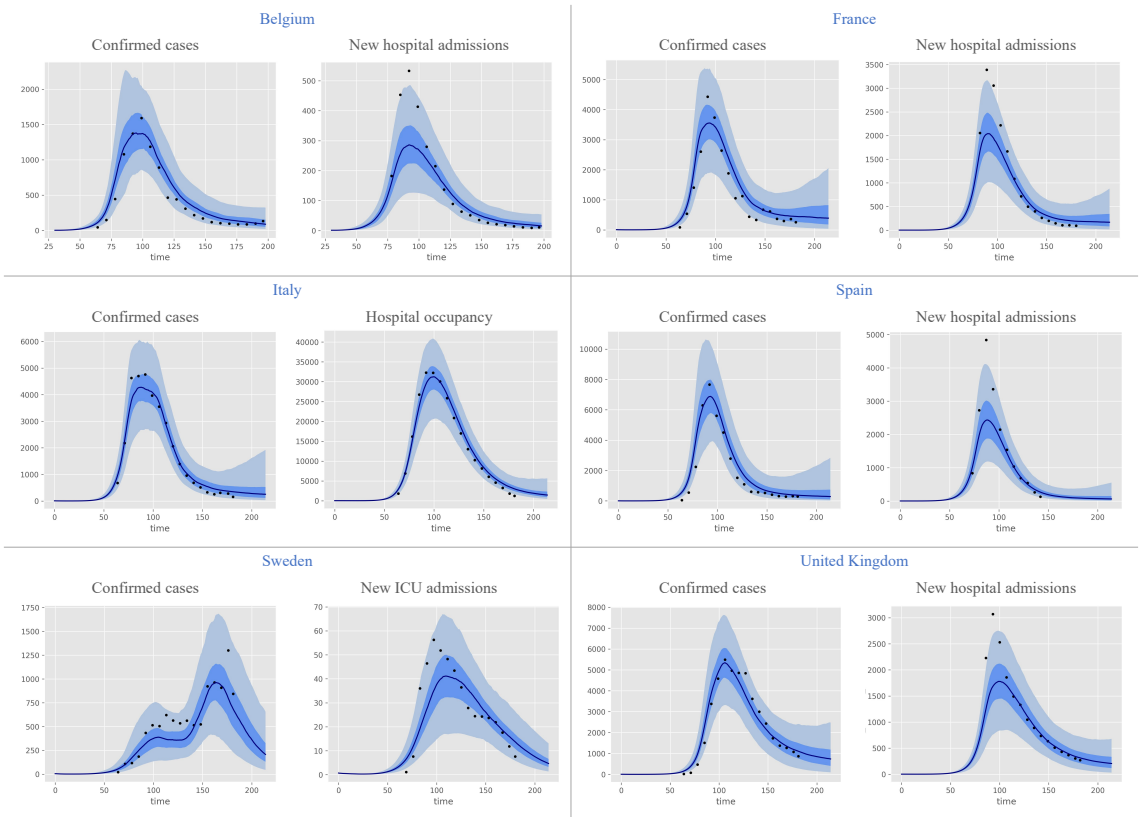

Figure 2. Model projections compared against local data
The figures present the median estimates (dark blue line) and the central 95% credible intervals (light blue shade) against observed numbers of confirmed COVID-19 cases and hospitalisations (black dots). The x-axis represents the time in days since 31/12/2019. Values on the y-axis are daily numbers of confirmed cases or hospitalisations. The data points represent the weekly average of the daily counts.

medRxiv preprint doi: https://doi.org/10.1101/2020.08.25.20182162; this version posted August 31, 2020. The copyright holder for this preprint **(which was not certified by peer review)** is the author/funder, who has granted medRxiv a license to display the preprint in perpetuity.
It is made available under a CC-BY-NC-ND 4.0 International license .

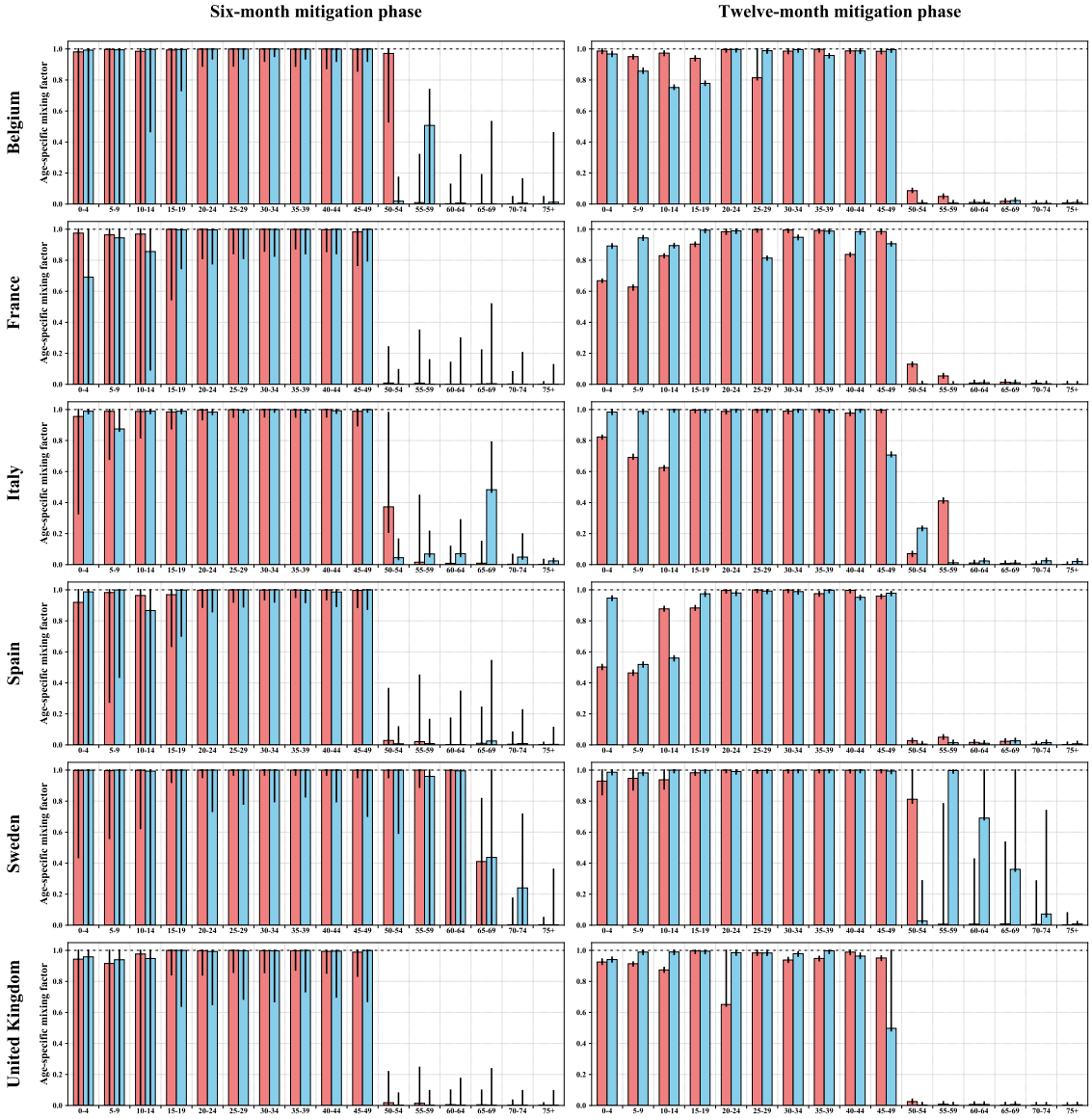

Figure 3. Optimal mixing pattern with contact mitigation by age
The red bars and the blue bars represent the optimised age-specific mixing factors when minimising the number of deaths and years of life lost, respectively. To determine the relative contact rate of one age category with another, the relative mixing values of each of the two categories must be multiplied together. The thin black bars represent the differential individual age-group contributions that would cause an excess of 20 deaths per million people (red bars) or 1000 YLLs per million people (blue bars) as compared to the optimal plan, while still reaching herd immunity by the end of the mitigation phase. The left and right panels show the result obtained when assuming that the mitigation phase lasts 6 and 12 months, respectively. The optimisations were performed based on the countries' maximum a posteriori parameter sets.

medRxiv preprint doi: https://doi.org/10.1101/2020.08.25.20182162; this version posted August 31, 2020. The copyright holder for this preprint (which was not certified by peer review) is the author/funder, who has granted medRxiv a license to display the preprint in perpetuity.
It is made available under a CC-BY-NC-ND 4.0 International license .

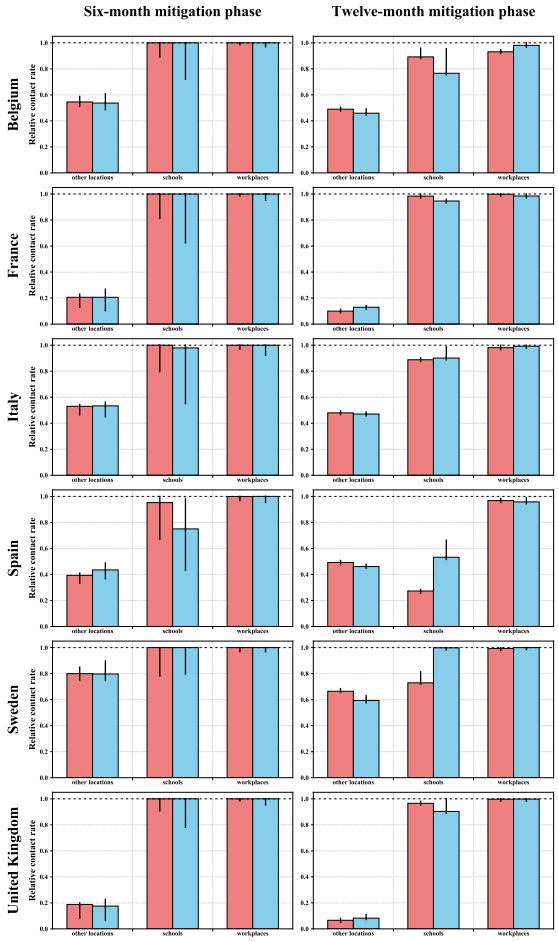

Figure 4. Optimal mixing pattern with contact mitigation by location
The red bars and the blue bars represent the optimised relative contact rates by location when minimising the number of deaths and years of life lost, respectively. The thin black bars represent the differential individual age-group contributions that would cause an excess of 20 deaths per million people (red bars) or 1000 YLLs per million people (blue bars) as compared to the optimal plan, while still reaching herd immunity by the end of the mitigation phase. The left panels show the result obtained when assuming that the mitigation phase lasts 6 months. In the right panels, a longer duration of 12 months was allowed to achieve herd immunity. The optimisations were performed based on the countries' maximum a posteriori parameter sets.

medRxiv preprint doi: https://doi.org/10.1101/2020.08.25.20182162; this version posted August 31, 2020. The copyright holder for this preprint **(which was not certified by peer review)** is the author/funder, who has granted medRxiv a license to display the preprint in perpetuity.
It is made available under a CC-BY-NC-ND 4.0 International license .

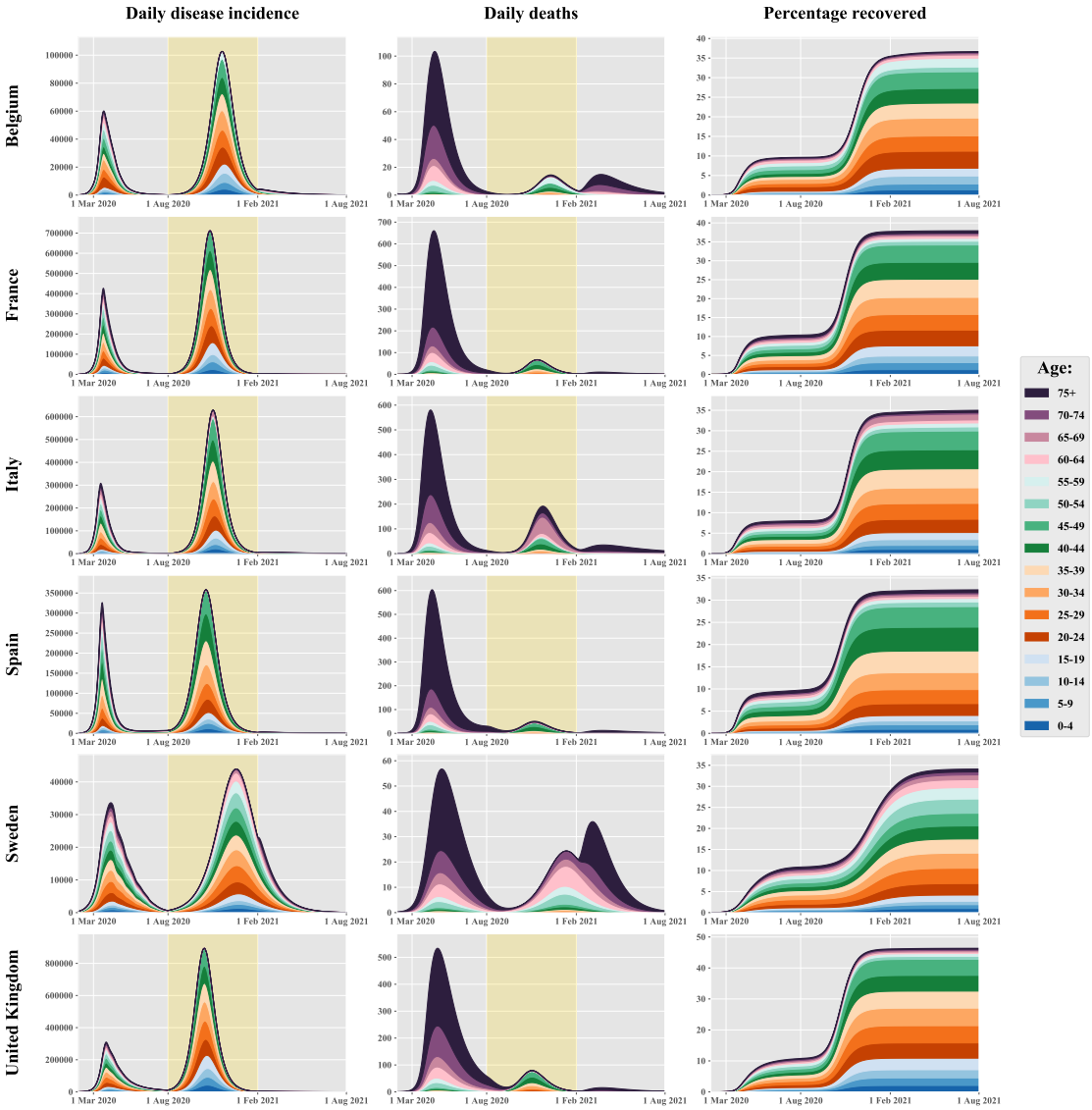

Figure 5. Age-specific profile of disease incidence, COVID-19-related deaths and proportion recovered over time optimised for life-years lost (6-month mitigation by age)

The yellow background indicates the 6-month mitigation phase during which age-specific contacts were optimised. These projections were produced assuming that recovered individuals have persistent immunity against SARS-CoV-2 reinfection and using the maximum a posteriori parameter sets.

medRxiv preprint doi: https://doi.org/10.1101/2020.08.25.20182162; this version posted August 31, 2020. The copyright holder for this preprint (which was not certified by peer review) is the author/funder, who has granted medRxiv a license to display the preprint in perpetuity.
It is made available under a CC-BY-NC-ND 4.0 International license .

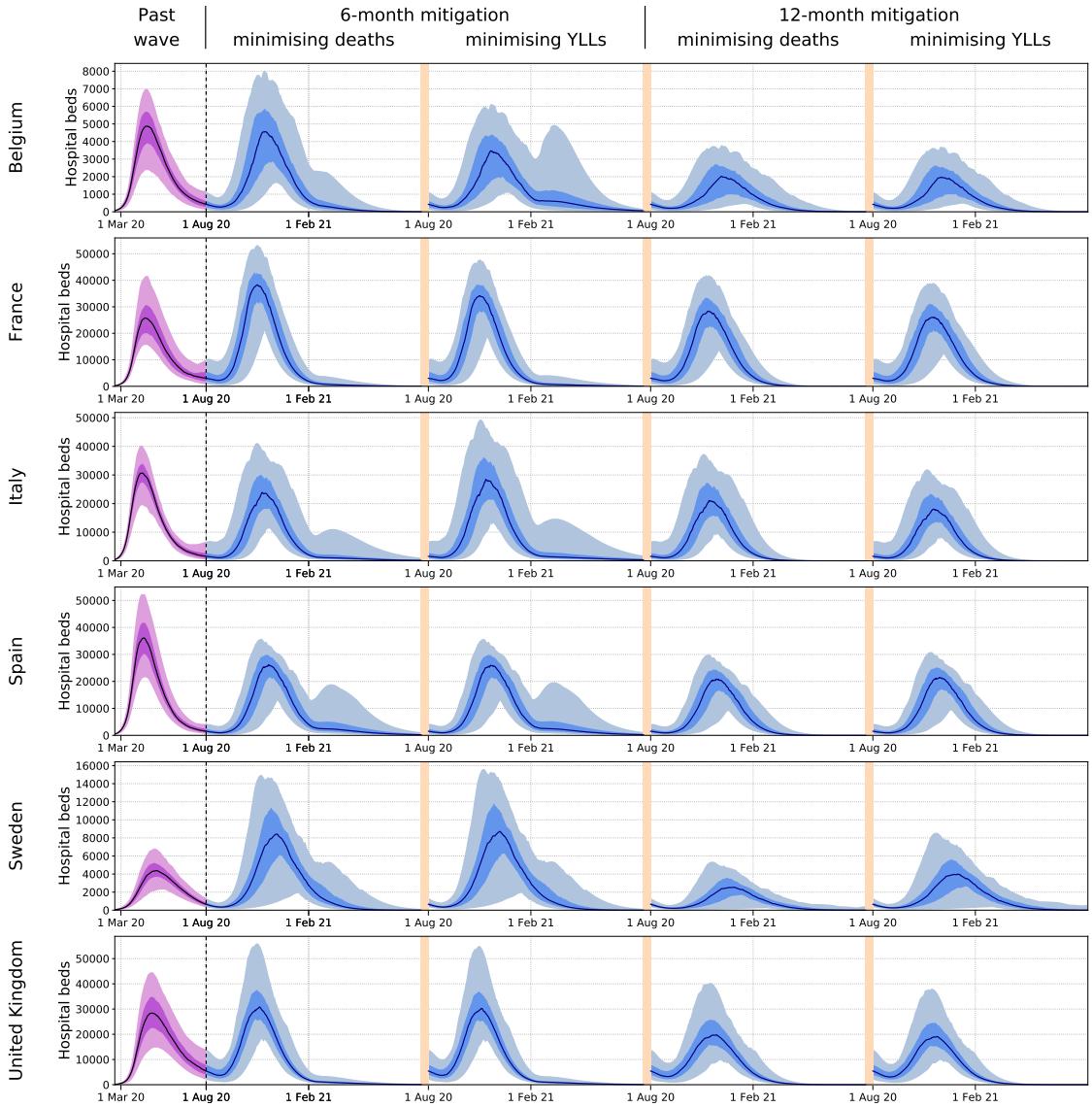

Figure 6. Predicted hospital occupancy during the past wave compared to a second wave that would achieve herd immunity (optimised mitigation by age, assuming persistent immunity)

The modelled first waves (past epidemics) are represented in purple while the predictions of the future epidemics are represented in blue. The future epidemics are those associated with the four different optimisation configurations: six- or 12-month mitigation minimising total number of deaths or years of life lost (YLLs). The light shades show the central 95% credible intervals, the dark shades show the central 50% credible intervals and the solid lines represent the median estimates.

medRxiv preprint doi: https://doi.org/10.1101/2020.08.25.20182162; this version posted August 31, 2020. The copyright holder for this preprint **(which was not certified by peer review)** is the author/funder, who has granted medRxiv a license to display the preprint in perpetuity.
It is made available under a CC-BY-NC-ND 4.0 International license .

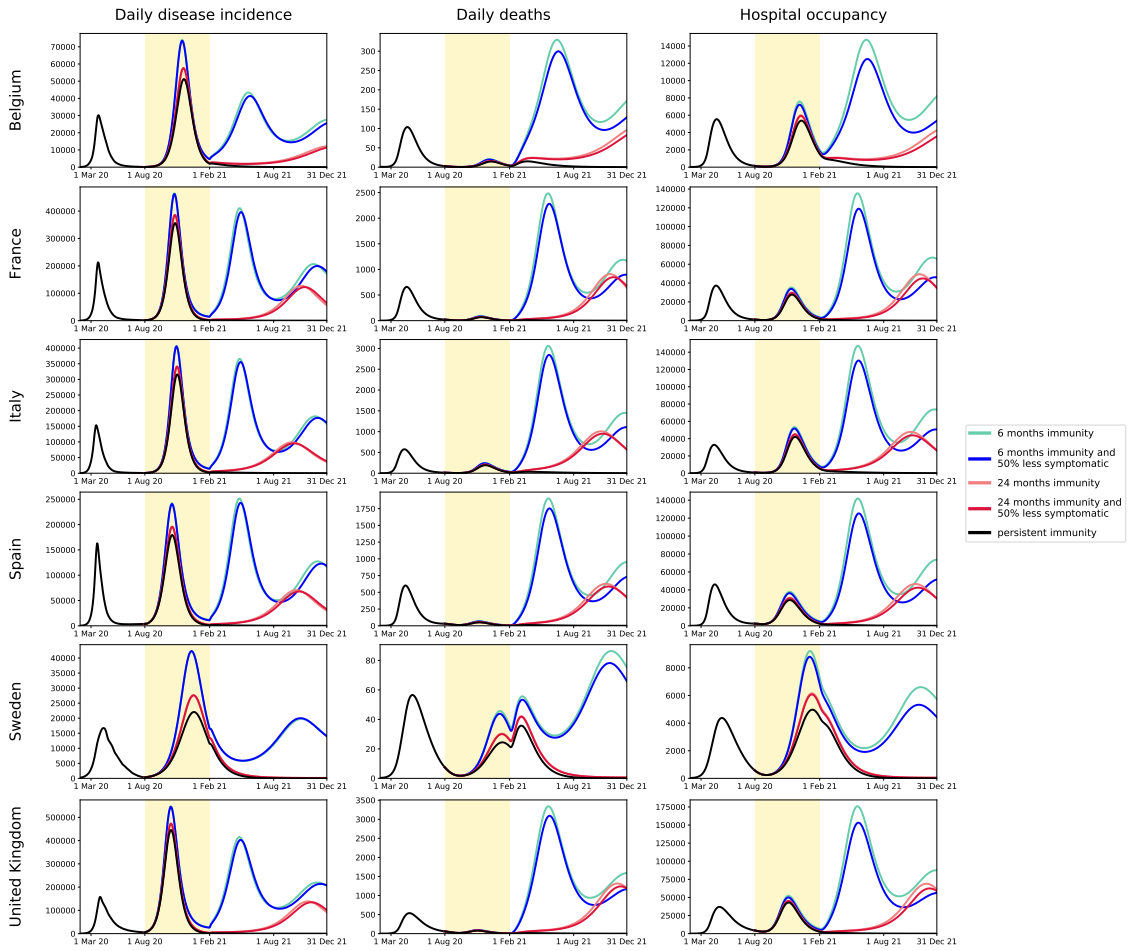

Figure 7. Predicted COVID-19 incidence, mortality and hospital occupancy over time under various assumptions of waning immunity

Predictions were obtained using the maximum a posteriori parameter sets and based on the 6-month contact mitigation by age minimising years of life lost (YLLs). The yellow background indicates the mitigation phase during which age-specific contacts were optimised. Five different assumptions were used to project the disease indicators: persistent immunity (black), 24-month average duration of immunity with and without 50% reduction in risk of symptoms for repeat infections (red and coral, respectively), 6-month average duration of immunity with and without 50% reduction in risk of symptoms for repeat infections (blue and turquoise, respectively).

medRxiv preprint doi: https://doi.org/10.1101/2020.08.25.20182162; this version posted August 31, 2020. The copyright holder for this preprint **(which was not certified by peer review)** is the author/funder, who has granted medRxiv a license to display the preprint in perpetuity.
It is made available under a CC-BY-NC-ND 4.0 International license .

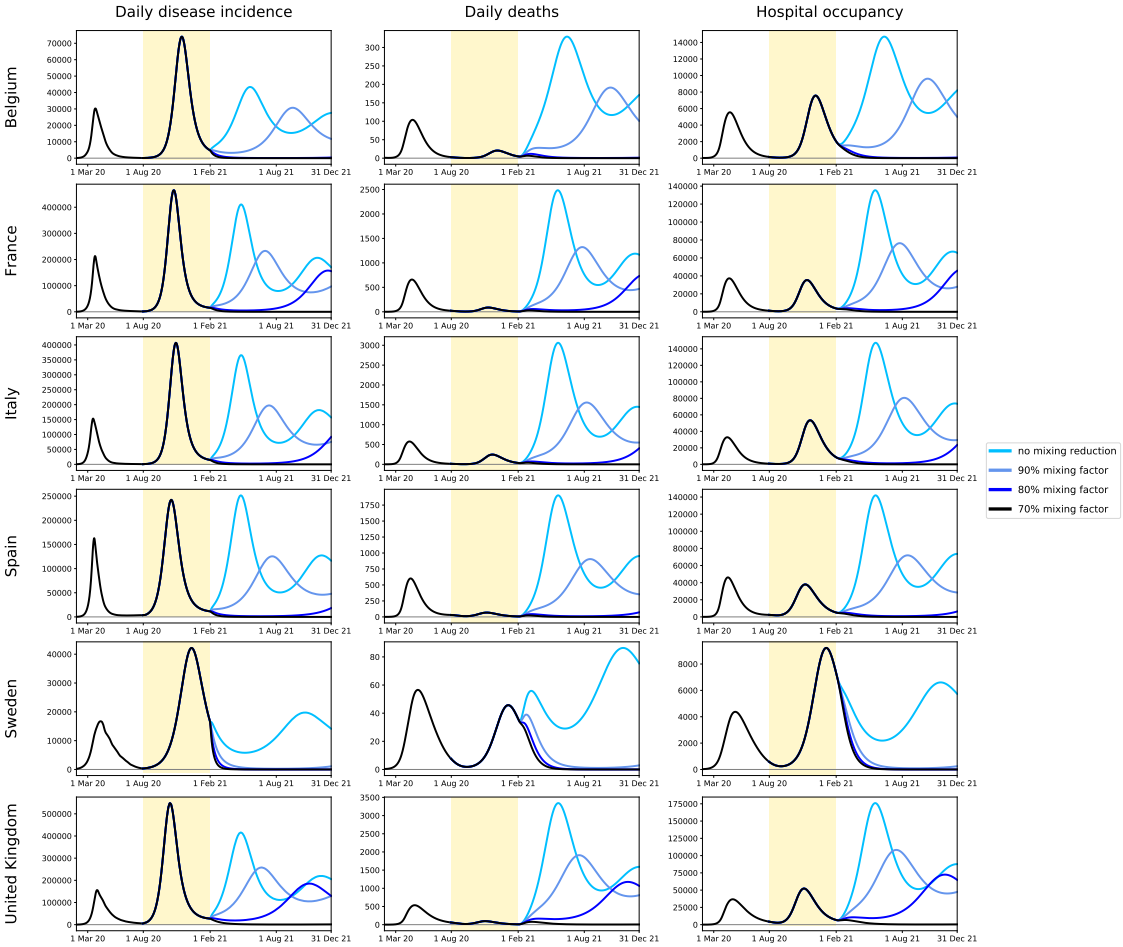

Figure 8. Predicted COVID-19 incidence, mortality and hospital occupancy over time with short-lived post-infection immunity and applying mild mixing reductions after the optimised phase

The predictions were obtained using the maximum a posteriori parameter sets and based on the 6-month contact mitigation by age minimising years of life lost (YLLs). The yellow background indicates the mitigation phase during which age-specific contacts were optimised. These predictions were obtained assuming 6-month average duration of immunity with no effect on the severity of repeat SARS-CoV-2 infections. The mixing factors were defined in the same way as during optimisation except that the same factor was applied to all age-groups. That is, a 90% mixing factor corresponds to a situation where every individual reduces their opportunity of contact by 10%.